Proc. Natl. Acad. Sci. USA
Vol. 86, pp. 9926–9930, December 1989
Cell Biology

Visualization of crystallin droplets associated with cold cataract formation in young intact rat lens

(scattering elements/opacification/morphology/young rat lens/immunoelectron microscopy)

WOO-KUEN LO

Department of Anatomy, Morehouse School of Medicine, 720 Westview Drive, S.W., Atlanta, GA 30310

Communicated by George B. Benedek, September 14, 1989

ABSTRACT **The structure, distribution, and nature of scattering elements associated with cold cataract formation in the young rat lens were studied *in situ* using light and electron microscopy and ImmunoGold electron microscopy. A large accumulation of spherical droplets, ranging from approximately 1.5 μm to 10 μm in diameter, were found in the lens nucleus in cold cataracts induced at 22°C or 4°C in TC-199 culture medium. Many droplets of all sizes were associated with the cell membranes. A cooled and then rewarmed lens was found to lose its opacity and subsequently no droplets were observed, indicating that there was a good correlation between the onset of opacification and the formation of droplets. Electron microscopy showed that droplets were composed of homogeneous electron-dense aggregates without limiting membranes. ImmunoGold study revealed that α-, β-, and γ-crystallins were all present within each droplet. This study demonstrates that extensive accumulation of the crystallin droplets in the lens nucleus is the contributing factor for the light scattering and opacification of the cold cataract in the young intact rat lens.**

The cold cataract can be induced in the nucleus of young mammalian lenses by low temperature (1–3). The critical temperature for cold cataract formation varies with the age and species of animal and can be altered by various conditions and factors (4–9). Under normal conditions, for example, the cold cataract occurs below 26°C in the lens nucleus of a 4-week-old rat (10), whereas it appears below 0°C in rat lenses at older ages (2). Also, the cold cataract can be reversed to its complete transparency by warming the lens above the opacification temperature.

Zigman and Lerman and colleagues (1, 4) have shown that the cold-precipitable protein fraction of rat lens contains three major crystallins, of which the relative concentrations for γ- α-, and β-crystallins are 65%, 23%, and 12%, respectively. Thus, γ-crystallins are considered to be the cryoprotein responsible for cold cataract formation in the young lenses (3, 4, 11). This notion is further supported by the findings that (*i*) there is a marked decrease in the relative concentration of γ-crystallins in the lens nucleus with age, which is consistent with the fact that the induction of cold cataract in an older lens requires a much lower temperature (1, 2), and (*ii*) purified γ-crystallins alone can be induced to form cold precipitates (2, 4). Moreover, recent studies indicate that γ-crystallin fraction IV is probably the primary determinant associated with cold opacification in the calf lens (11–13).

Benedek and coworkers (3, 8, 14–17) have suggested that the formation of cold cataract is due to a phase-separation phenomenon. When phase separation occurs at or below opacification temperature, both protein-rich and protein-poor phases are believed to be produced in the nuclear cytoplasm. The concentration fluctuation responsible for the scattering contains several different sizes of scattering elements, as detected in opacifying calf lens, isolated nuclear cytoplasm, and purified γ-crystallin solutions by using quasi-elastic light-scattering spectroscopy (11, 12, 16).

Identification of the structure of the scattering elements has been attempted in the cytoplasmic extracts of calf lens by freeze-fracture electron microscopy (18). However, the structural basis by which the lens crystallins cause light scattering in the cold cataracts has never been demonstrated in the intact lens of any species. Also, it is not clear whether the three major crystallins are all involved in the *in vivo* formation of the scattering elements in the cold cataract. In this study, I describe the structural characteristics, spatial distribution, and nature of scattering elements that uniquely correlate with cold cataractogenesis in the intact lens of the young rat, using light and electron microscopy and ImmunoGold electron microscopy.

MATERIALS AND METHODS

Light and Electron Microscopy. Approximately 50 lenses from postnatal Sprague–Dawley rats, 1–14 days of age, were used in this study. Rats anesthetized by ether were decapitated and their eyes were removed. Freshly enucleated lenses were then kept in TC-199 culture medium at room temperature (22°C) or 4°C. "Cold cataracts" of these young lenses were formed below 28°C in TC-199. However, cold cataracts of young lenses were also observed at 22°C in the enucleated eye balls before placing in TC-199 medium. Thus, in this study the cold cataracts were induced and fixed at 22°C and 4°C to investigate the possible differences in the structure and distribution of the scattering elements. All lenses were fixed in an improved fixation mixture containing 2.5% glutaraldehyde/0.1 M sodium cacodylate buffer (pH 7.3), 50 mM L-lysine, and 1% tannic acid (19) for 2–4 hr. Animals used as controls were kept warm by a minielectric blanket before decapitation. Transparent lenses were rapidly removed and fixed at 37°C for 2 hr in the same fixation mixture. Some cold cataracts were reversed several times between 22°C and 37°C (each for 15–30 min) in TC-199 medium. Opacifying lenses formed at 22°C were then fixed at 22°C, whereas transparent lenses maintained at 37°C were fixed at 37°C to study the correlation between the onset of opacification and the formation of scattering elements. Fixed lenses were then cut into halves with a razor blade or cut into 400-μm serial slices with a Vibratome (Lancer, Saint Louis). Lens slices were fixed for an additional 2 hr in the fixation mixture, postfixed in 1% aqueous OsO_4 for 1–2 hr at 22°C, dehydrated in ethanol and propylene oxide, and embedded in Polybed 812 resin (Polysciences). Thick sections (1–1.5 μm) were stained with azur/methylene blue or toluidine blue and examined with a light microscope. A small area of deep cortex and nucleus was cut for thin-section electron microscopy. Ultrathin sec-

The publication costs of this article were defrayed in part by page charge payment. This article must therefore be hereby marked "*advertisement*" in accordance with 18 U.S.C. §1734 solely to indicate this fact.

tions (80 nm) were stained with uranyl acetate and Reynold's lead citrate and examined with an electron microscope.

ImmunoGold Electron Microscopy. The young lenses with cold cataracts formed at 22°C were fixed in the glutaraldehyde fixation mixture or in 2% paraformaldehyde and 1.25% glutaraldehyde/0.1 M sodium cacodylate buffer (pH 7.3), for 1–2 hr. Lens slices were prepared and dehydrated in graded ethanol and embedded in LR-White embedding medium (Polysciences). Ultrathin sections were cut with a diamond knife and collected on nickel grids. Blocking of nonspecific IgG in the sections was done in a blocking solution containing 5% dry milk/1% bovine serum albumin (BSA)/phosphate-buffered saline (PBS), pH 7.3, for 2 hr. Sections were incubated on droplets of the bovine polyclonal antibodies to α-, β- and γ-crystallins at full strength overnight at 4°C. All antibodies were kindly provided by Samuel Zigler (National Eye Institute, National Institutes of Health). Crystallins were separated by chromatography on Sephadex G-200, and the individual peaks were purified by rechromatography on the same or similar gel filtration medium. Antisera were produced in rabbits with immunizations at 14-day intervals. Antisera were tested for specificity by immunodiffusion and Western blotting (20). Following incubation, the grids were washed with PBS (6 × 1 min) and blocked again with the blocking solution for 1 hr. Sections were incubated for 1 hr on droplets of biotinylated goat anti-rabbit IgG (Bethesda Research Laboratories), diluted 1:100 with 1% BSA/PBS, pH 7.3, and washed with PBS (6 × 1 min). The grids were finally incubated for 1 hr on droplets of streptavidin/10-nm gold (Janssen Pharmaceutica), diluted 1:50 with 1% BSA/PBS, pH 7.3. Grids were washed with PBS (6 × 1 min) followed by distilled water (12 × 1 min), stained with 5% uranyl acetate and Reynold's lead citrate, and examined with a JEOL 1200EX electron microscope. Controls were processed in the same manner except preimmune rabbit serum was used to substitute for the primary antibodies or the primary antibodies were omitted. Both types of controls were used to evaluate the specificity of ImmunoGold labeling for the antibodies.

RESULTS

Visualization of the Scattering Elements. Fig. 1 shows that a 13-day-old lens exhibits dense nuclear opacity at 22°C but shows transparency at 37°C in TC-199 medium. In all young lenses studied, opacity was observed below 28°C in TC-199. Young lenses also showed the formation of nuclear opacities in the enucleated eye balls at 22°C. A stereo dissecting microscopy revealed that the opacity was initiated in the form of a perinuclear ring, ≈300 μm deep from the equatorial capsule surface. The width of the ring subsequently expanded inward to the nuclear core and outward to the cortical regions. Some were found extended to superficial cortical areas along the anterior and posterior sutures. The speed of opacity expansion for the entire lens nucleus of very young lenses needed only a few seconds at 4°C.

Light microscopy showed that a tremendous number of spherical structures, resembling "droplets," were accumulated in the nucleus of the cold cataract (Fig. 2*A*). The term "droplet" is therefore used to designate these structures. A cooled and then rewarmed lens was found to lose its opacity, and subsequently no droplets were observed (Fig. 2*B*). Also, droplets were never seen in the transparent lenses that were kept warm throughout the experimental period. At higher magnification, the droplets in the cold cataract were found distributed in the cytoplasm of every nuclear fiber cell (Figs. 3 and 4). Most droplets were spherical or oval in shape, with various sizes ranging from approximately 1.5 μm to 10 μm in diameter. The size range of the droplets was determined in serial thick sections (1.5 μm in thickness) in which the same droplets were traced and measured in the light micrographs. In most cases, a distinct group of small-sized droplets (about 1.5 μm in diameter) was always found in serial sections at the outermost region of opacity defined by the perinuclear ring (Figs. 2*A* and 3), whereas larger droplets (up to about 10 μm) were seen in the same sections in the deeper regions of the lens (Fig. 3). In a few cases, however, many larger droplets with a similar size (about 3 μm) were found at the most superficial region of the opacities that had been reversed several times and incubated for a longer period of time (Fig. 4). In addition, a majority of these small droplets (Fig. 3) and many larger ones (Figs. 3 and 4) were found closely associated with the cell membranes. The distribution of droplets in the cold cataracts induced at 4°C extended to a more superficial region of the deep cortex as compared to those formed at 22°C. Some droplets were even visualized along the anterior suture up to the apical surface of the lens epithelium (data not shown).

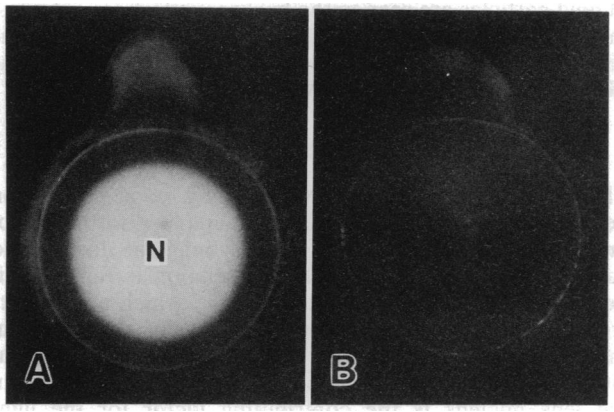

FIG. 1. A 13-day-old rat lens kept in TC-199 medium at different temperatures. (*A*) At 22°C, heavy opacity is found in the entire lens nucleus (N). (*B*) At 37°C, the nuclear opacity of the same lens is lost, and the whole lens becomes transparent. The diameter of the lens is 3.0 mm.

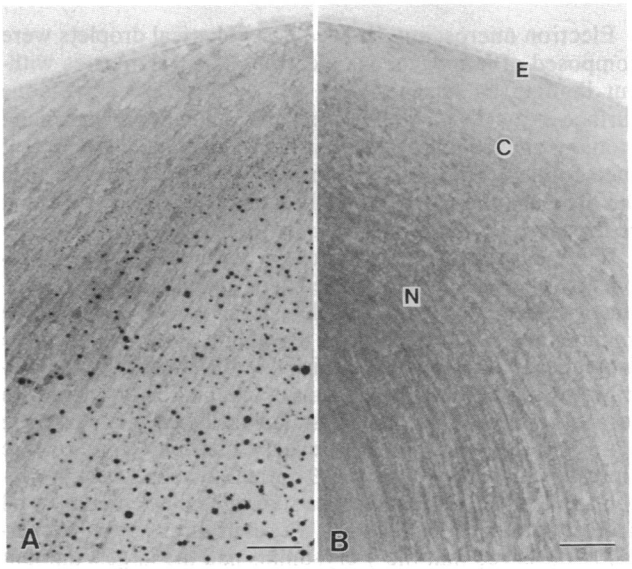

FIG. 2. Overview of a portion of a cold cataract and transparent control for morphological comparison. (*A*) Cold cataract formed at 22°C shows that numerous dense droplets are distributed in the nuclear region, indicating a good spatial correlation with the onset of opacity. (*B*) Transparent lens after reversal from the cold cataract by warming to 37°C shows no droplets in the entire lens. E, epithelium; C, cortex; N, nucleus. (Bars = 50 μm.)

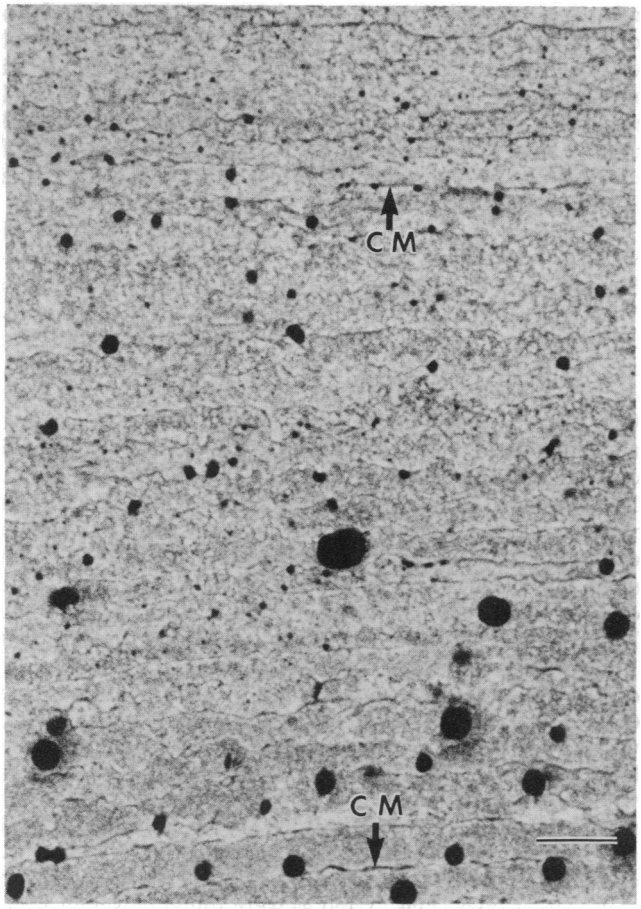

FIG. 3. Light micrograph of cold cataract formed at 22°C showing distribution of different sizes of droplets in fiber cells. A distinct zone of small-sized droplets (about 1.5 μm in diameter) is commonly seen at the most superficial region close to the cortex at top, whereas large droplets are distributed in a deeper area near the nucleus at bottom. Note that many small droplets and some large ones are closely associated with the cell membrane (CM). (Bar = 15 μm.)

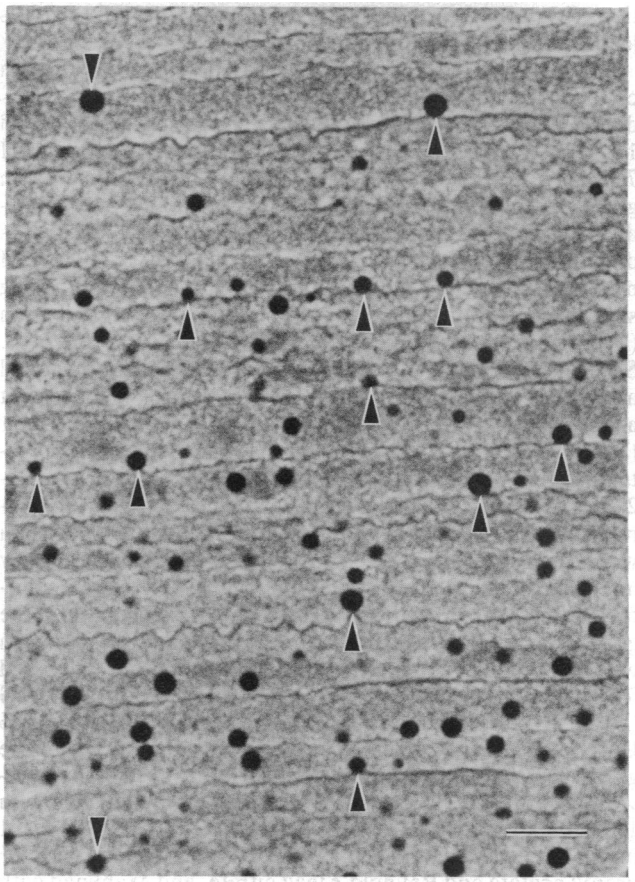

FIG. 4. Light micrograph of cold cataract of 4-day-old lens that had been reversed several times between 37°C and 22°C and was finally incubated for 1 hr at 22°C before fixation. Spherical droplets of a relatively large and even size (about 3 μm in diameter) are seen at the outermost area of perinuclear ring defined by opacity. Close associations between droplets and cell membranes are indicated by arrowheads. (Bar = 10 μm.)

Electron microscopy showed that spherical droplets were composed of homogeneous electron-dense aggregates without limiting membranes (Fig. 5). A close contact of one surface of the droplets with the plasma membrane was found in many electron micrographs. Fig. 5 shows an example of such contact. This observation of the close contact between the droplets and the cell membranes is consistent with that observed in the light micrographs (Figs. 3 and 4).

ImmunoGold Identification of the Nature of Scattering Elements. The ImmunoGold labeling of the antibodies to α-, β- and γ-crystallins in the droplets is shown in Fig. 6. The immunolabel of these three crystallins was seen in the droplets. There are some noticeable differences in the distribution pattern and the amount of label in the droplets with respect to three individual crystallin antibodies. The labeling of α- and γ-crystallins was evenly distributed within the entire droplets, whereas the β-crystallins showed more labeling along the peripheral area than the center of almost all droplets studied (Fig. 6*A–C*). Furthermore, it was consistently observed that the γ-crystallins had the largest amount of label in the droplets, whereas the β-crystallins showed the smallest. The labeling pattern of the three crystallin antibodies appeared to be the same in the droplets located in the cortex as those in the nucleus of the lens. Also, the small-sized droplets at the outermost region of lens opacity had the same labeling pattern as the large ones distributed in a deeper location (data not shown). In both controls for ImmunoGold labeling, there were no appreciable gold particles found in the droplets and cytoplasm. Fig. 6*D* shows a droplet without gold label in the absence of the primary antibodies. In addition, the difference in the amount of label in the inside vs. outside of the droplets is sometimes discernible, particularly in the case of β-crystallins. The outside cytoplasmic materials appear to exhibit more label for β-crystallins than the center of the droplets (Fig. 7). Fig. 7 also shows that only a small number of gold particles are seen in the background where cytoplasmic materials are not present, suggesting that nonspecific binding of antibodies has been greatly reduced after using the blocking solution in the LR-White-embedded tissue.

DISCUSSION

This study demonstrates that there is a good correlation between the onset of opacification and the formation of droplets in the lens nucleus of the young rat during cold cataract formation *in situ*. This correlation is further evidenced by the reversible experiments in which no droplets were seen in the transparent lenses following reversal from the cold cataract by warming. Thus, the extensive accumulation of spherical droplets (about 1.5–10 μm in diameter) in the lens nucleus is the contributing factor for the light scattering and opacification of the cold cataract.

The ImmunoGold study shows that each droplet in the intact lens is composed of α-, β- and γ-crystallins, which is consistent with the results obtained by an immunodiffusion method in the purified cold-precipitable fraction of the young

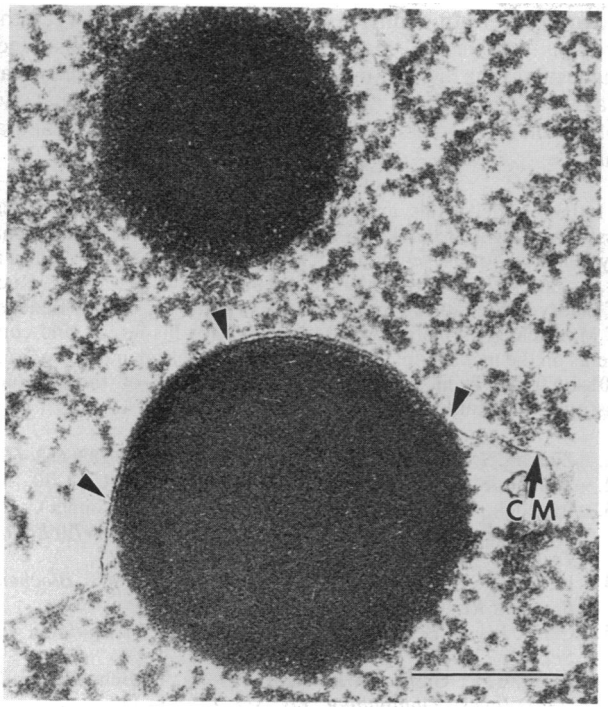

FIG. 5. Electron micrograph of droplets showing the homogeneous nature of an electron-dense aggregate. No limiting membrane is seen to encircle the outer surface of droplets. Close contacts between the surface of a droplet and the cell membrane are indicated by arrowheads. CM, cell membrane. (Bar = 1 μm.)

rat lens (2). This study, however, does provide more definite information about the involvement of the three major crystallins in the *in situ* formation of individual scattering elements (droplets) responsible for opacification in cold cataract.

The ImmunoGold study also shows that the labeling pattern of the three crystallins is the same in the small droplets as in the large ones. This is evidenced by the observations from the group of small droplets at the outermost region of opacity as compared to the large droplets in the deeper nuclear area. These results suggest that droplets of all sizes may be formed by a consistent process in which a specific labeling pattern of three individual crystallins in the droplets can be maintained. Because the formation and dissociation of droplets can occur within a considerably short period of time (e.g., a few seconds at 4°C and 37°C, respectively) as a function of the critical temperature, each of the three crystallins is perhaps able to be mobilized or rearranged rapidly for this purpose.

How the large droplets are formed is not clear. Based on the observation that many larger droplets can be induced at the outermost region of the opacity by increased incubation time (Fig. 4), it is possible that the large droplets are formed by the addition of new materials to the surface of small droplets as a function of time in a given opacification temperature. Direct contact and fusion between two droplets were rarely observed, suggesting that large droplets may not be formed by means of this mechanism.

Another unique feature of the droplets is that almost all of the small droplets seen at the outermost regions of opacity are closely associated with cell membranes (Fig. 3). It is reasonable to suggest that the cell membrane perhaps serves as an initiation surface in the early phase of droplet formation. Because close associations are also found between the larger droplets and the cell membranes (Figs. 3 and 4), it is possible that the cell membrane may subsequently serve as an anchoring site for the later phase of large droplet development.

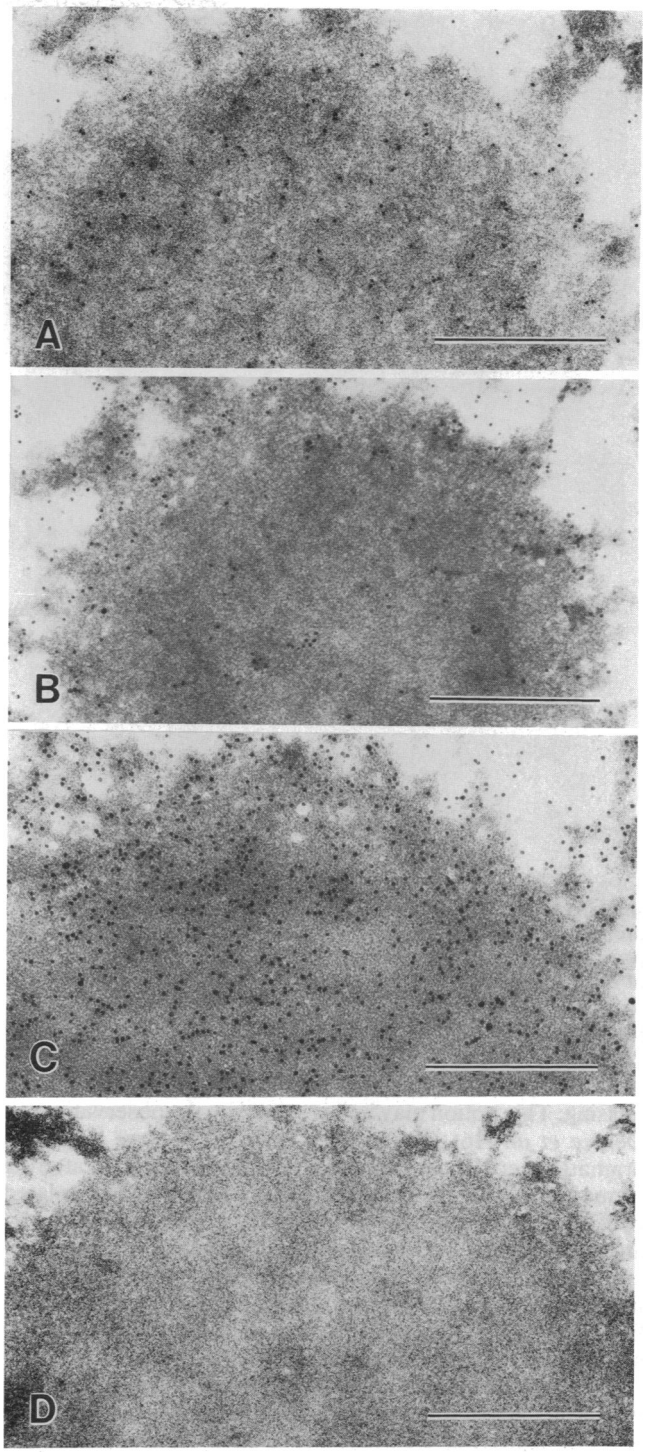

FIG. 6. ImmunoGold electron micrograph showing labelings of polyclonal antibodies to α-, β- and γ-crystallins in the droplets formed at 22°C from 3-day-old rat lens. (*A*) Anti-α-crystallins. Gold particles (10 nm) are evenly distributed throughout the droplet. (*B*) Anti-β-crystallins. Only a sparse labeling is seen inside the droplet, whereas more gold particles are scattered at the edge and peripheral area. (*C*) Anti-γ-crystallins. A heavy and even localization of this antibody is shown within the entire droplet. (*D*) Control, in which the primary antibodies were omitted, shows no labeling of gold particles in the droplet. (Bar = 0.5 μm.)

The importance of the cell membrane in this respect may be heightened by the fact that there are not other membranous organelles within the nuclear fiber cells (21–23) that would serve the same purpose. Thus, the presence of organized cell-membrane domains in the intact lens may play an im-

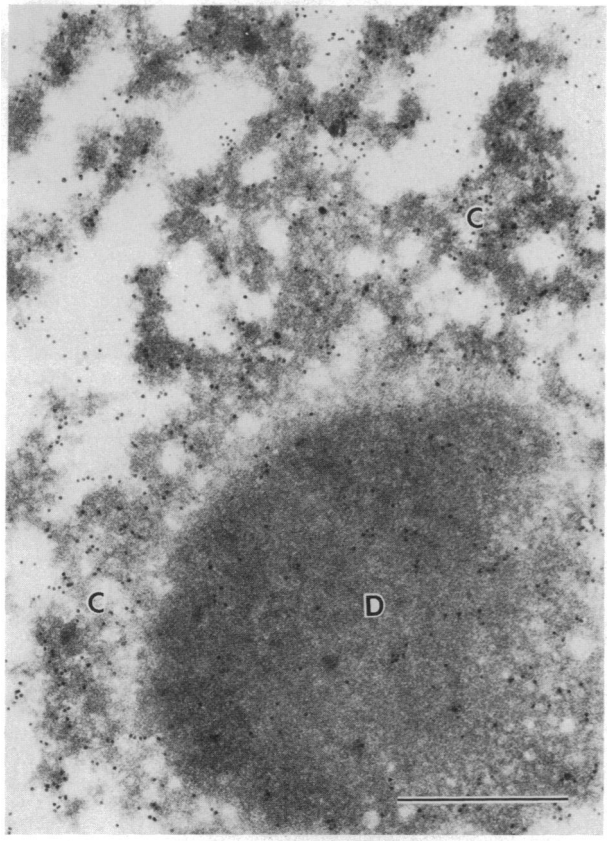

FIG. 7. ImmunoGold labeling of the antibody to β-crystallins showing a noticeable difference in the amount of label over the droplet compared to the surrounding cytoplasmic materials. It appears that cytoplasmic materials (C) have more labeling than the core of the droplet (D). (Bar = 0.5 μm.)

portant role during a rapid increase in the droplet size, in contrast to those formed in cytoplasmic extracts and γ-crystallin solutions in which the intact cell membranes are missing. This notion may be supported by the observations of Delaye *et al.* (16). Their studies show that there is a more dramatic increase in the mean size of the large scattering elements in the intact lens nucleus than in the isolated cytoplasm when both are reaching the cold cataract temperature, as detected by quasielastic light-scattering spectroscopy. The present study also reveals that the size of some large droplets (up to 10 μm in diameter) found in the intact fiber cells is much greater than those estimated in γ-crystallin solutions or cytoplasmic extracts (11, 16, 18).

In conclusion, spherical droplets (≈1.5–10 μm in diameter) within all nuclear fiber cells and some deep cortical fiber cells are the scattering elements associated with cold cataract opacification. Each droplet contains α-, β-, and γ-crystallins as determined by ImmunoGold labeling of the three individual antibodies. In addition, a close association between the droplets and the cell membranes was frequently observed, suggesting that the cell membranes of intact fiber cells may play an important role as initiation surfaces during the *in vivo* formation of droplets in response to cold cataract temperature.

I thank Adell Mills and Muriel Gavin for excellent technical assistance. Special thanks go to Dr. Samuel Zigler of the National Eye Institute for his generous gift of bovine polyclonal antibodies to α-, β-, and γ-crystallins. Valuable assistance from Dr. John F. Kuck of Emory University is appreciated. I also thank Dr. George Benedek of Massachusetts Institute of Technology for his advice and comments on the manuscript. This study was supported in part by Grant R01-EY05314 from the National Eye Institute of the National Institutes of Health.

1. Zigman, S. & Lerman, S. (1964) *Nature (London)* **203**, 662–663.
2. Zigman, S. & Lerman, S. (1965) *Exp. Eye Res.* **4**, 24–30.
3. Benedek, G. B., Clark, J. I., Serrallach, E. N., Young, C. Y., Mengel, L., Sauke, T., Bagg, A. & Benedek, K. (1979) *Philos. Trans. R. Soc. London Ser. A* **293**, 329–340.
4. Lerman, S., Zigman, S. & Forbes, W. F. (1966) *Biochem. Biophys. Res. Commun.* **22**, 57–61.
5. Clark, J. I. & Benedek, G. B. (1980) *Invest. Ophthalmol. Vis. Sci.* **19**, 771–776.
6. Clark, J. I., Giblin, F. J., Reddy, V. N. & Benedek, G. B. (1981) *Invest. Ophthalmol. Vis. Sci.* **22**, 186–190.
7. Clark, J. I., Neuringer, J. R. & Benedek, G. B. (1983) *J. Gerontol.* **38**, 287–292.
8. Hammer, P. & Benedek, G B. (1983) *Curr. Eye Res.* **2**, 809–814.
9. Siezen, R. J., Coppin, C. M. & Benedek, G. B. (1985) *Biochem. Biophys. Res. Commun.* **133**, 239–247.
10. Mizuno, A., Ozaki, Y., Itoh, K., Matsushima, S. & Iriyama, K. (1984) *Biochem. Biophys. Res. Commun.* **119**, 989–994.
11. Siezen, R. J., Fisch, M. R., Slingsby, C. & Benedek, G. B. (1985) *Proc. Natl. Acad. Sci. USA* **82**, 1701–1705.
12. Siezen, R. J. & Benedek, G. B. (1985) *Curr. Eye Res.* **4**, 1077–1085.
13. Siezen, R. J., Thomson, J. A., Kaplan, E. D. & Benedek, G. B. (1987) *Proc. Natl. Acad. Sci. USA* **84**, 6088–6092.
14. Clark, J. I. & Benedek, G. B. (1980) *Biochem. Biophys. Res. Commun.* **95**, 482–489.
15. Delaye, M., Clark, J. I. & Benedek, G. B. (1981) *Biochem. Biophys. Res. Commun.* **100**, 908–914.
16. Delaye, M., Clark, J. I. & Benedek, G. B. (1982) *Biophys. J.* **37**, 647–656.
17. Tanaka, T., Ishimoto, C. & Chylack, L. T. (1977) *Science* **197**, 1010–1012.
18. Gulik-Krzywicki, T., Tardieu, A. & Delaye, M. (1984) *Biochim. Biophys. Acta* **800**, 28–32.
19. Lo, W.-K. (1988) *Cell Tissue Res.* **254**, 31–40.
20. Zigler, J. S., Jr., & Sidbury, J. B., Jr. (1976) *Comp. Biochem. Physiol. B* **53**, 349–355.
21. Rafferty, N. S. (1985) in *The Ocular Lens*, ed. Maisel, H. (Dekker, New York), pp. 1–60.
22. Kuwabara, T. (1975) *Exp. Eye Res.* **20**, 427–443.
23. Maisel, H., Harding, C. V., Alcala, J. R., Kuszak, J. & Bradley, R. (1981) in *Molecular and Cellular Biology of the Eye Lens*, ed. Bloemendal, H. (Wiley, New York) pp. 49–84.